

## Micro-Raman Spectroscopy and Cathodoluminescence Study of Cross-section of Diamond Film

ChunLei Wang\*, Akimitsu Hatta, Jaihyung Won, Nan Jiang, Toshimichi Ito,  
Takatomo Sasaki, Akio Hiraki, Zengsun Jin\* and Guangtian Zou\*

Department of Electrical Engineering, Osaka University, Suita, Osaka 565, Japan

\*State Key Lab. of Superhard Materials, Jilin University, P.R. China

(Received November 5, 1996)

---

Diamond film (24  $\mu\text{m}$ ) were prepared by Microwave Plasma Chemical Vapor Deposition method from a reactive CO/H<sub>2</sub> mixtures. Micro-Raman spectroscopy and micro-cathodoluminescence study were carried out along the cross-section and correlated to SEM observation. CL image of cross-section was also investigated. Peak position, FWHM of Raman spectrum were determined using Lorentzian fit. The stress in this sample is 0.4-0.7 GPa compressive stress, and along the distance the compressive stress reduced. The Raman peak broadening is dominated by phonon life time reduction at grain boundaries and defect sites. Defects and impurities were mainly present inside the film, not at Silicon/Diamond interface.

**Key words :** CVD diamond film, Micro-Raman spectroscopy, Cathodoluminescence, Compressive stress, Defects and impurities

---

### I. Introduction

CVD diamond has attracted much interest because of its excellent physical and mechanical characterization and many different applications to optical and electronic devices. Knowledge about the origins and characteristics of stress and distributions of defects and impurities in diamond films is critical to grow pure diamond in low defect and impurity densities. Raman spectroscopy has proven to be one of the most useful techniques for analyzing diamond films. It is not only used to distinguish diamond from other forms of carbon, but also used to obtain information about stress type and magnitude, defect and impurity distribution in the diamond by investigating the full width at half-maximum (FWHM) and shift of the first-order diamond Raman line.<sup>1,2</sup> L.J. Bernardes *et al.*<sup>3</sup> performed measurement of CVD diamond by in situ Raman spectroscopy system, showed that the linewidth decreased with the growth and the film is under compressive stress. Stephanie R. Sails *et al.*<sup>4</sup> investigated stress and crystallinity variations along the growth direction in three diamond films of different preferred orientations, and found that the peak position and FWHM of <110> and <111> orientations showed random variation throughout. Cathodoluminescence has been proven to be one of the most successful techniques for characterizing defects and impurities in diamond. Among the luminescent centers observed in CVD diamond, band A, which attributed to dislocations,<sup>5</sup> is the major band. Kawarada *et al.*<sup>6</sup> have studied the CL image of CVD diamond and natural diamond, and found

CL image dependent on the growth sectors, {100} sectors and luminescent, but {111} sectors are not. They attributed the mosaic patterns of natural diamond to single dislocations in the crystal. Even though, the information about the cross-section of CVD diamond film is still far from sufficient. In this work, we deposit a 24  $\mu\text{m}$  thick diamond film by MWPCVD method. The detail of cross-section was investigated by micro-Raman spectroscopy and cathodoluminescence study.

### II. Experimental Procedure

Diamond film was deposited by means of microwave plasma assisted CVD deposition method. Substrate was (100) surface-oriented p-type silicon wafer. Before the deposition, it was pretreated by ultrasonically scratching with high pressure synthesized diamond powders. The plasma consisted of 10% CO in H<sub>2</sub> at 100 sccm total flowrate. The plasma power, pressure and substrate temperature were maintained at 250 W, 45 mbar and 930°C respectively. The sample was about 24  $\mu\text{m}$  thick measured by SEM.

Raman microspectroscopy has been carried out at room temperature using 514.5 nm argon ion laser line and recorded with a Dilor Laser Raman Modular XY spectrometer. Laser power, which be focused on a spot size about 1  $\mu\text{m}$  in diameter, was about 10 mW on the sample from  $\times 100$  microscope objective. The laser light was incident normal to the surface and scattered light was collected in 180° backscattering geometry mode. A natural diamond was used to calibrate the diamond line

at  $1331.2\text{ cm}^{-1}$ , with FWHM about  $3.6\text{ cm}^{-1}$ . All Raman measurements were taken in the same sitting for consistency of measurement. To get a quantitative analysis of first order diamond raman line, Lorentzian fitting was applied to each spectrum after subtract non linear background. The peak position and full width at half maximum (FWHM) were determined. A JSM-840 scanning electron microscope was used to measure the CL intensities of diamond film. In order to get the same spacial resolution as Raman microspectroscopy, the SEM accelerating voltage was fixed to 20 KV and the probe current was  $3 \times 10^{-8}\text{ A}$ . The observations were made at 80 K. For the cross-section study, the PSCAN mode was used, and scanning area was about  $1 \times 0.8\text{ }\mu\text{m}$ . CL image was taken at the same condition, with scanning area  $40 \times 30\text{ }\mu\text{m}$ .

### III. Results and Discussion

The diamond film used in this study is dominated by  $\langle 111 \rangle$  texture. The cross-section SEM image of this sample is presented in Fig. 1. Micro-Raman spectra were obtained from different points (A, B, C, D, E) at every  $6\text{ }\mu\text{m}$  from the silicon/diamond interface to diamond/air interface along six different individual crystal. Figure 2(a) is the typical three Raman spectra along one crystal. As can be seen from it, at position A, there is only first order diamond Raman peak with lower luminescent background; at position E near growth surface, the diamond Raman peak is sharper than which in position A; at position C, there are not only first order diamond Raman line but also some other peaks, as well as higher luminescent background which indicate a higher density of radiative defect centers in the film. Detail of the spec-

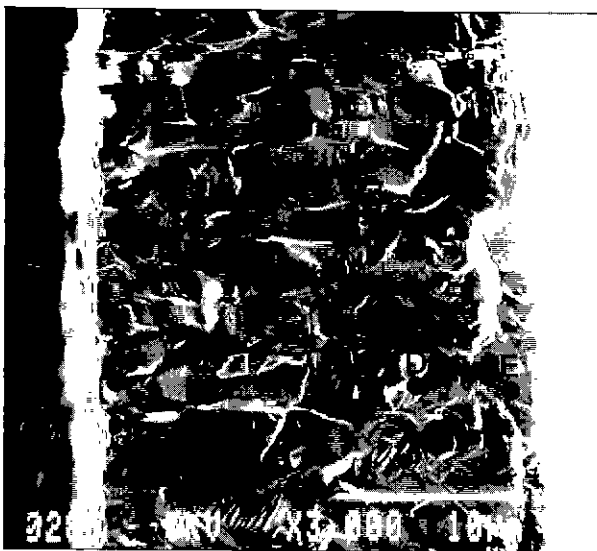


Fig. 1. The SEM micrographs of the cross-section of diamond film (A, B, C, D, E were typical six positions used in micro-Raman spectroscopy investigation).

trum C in Fig. 2(a) was shown in Fig. 2(b). The dash line curves are five Lorentzian fit peaks, and the open circle curve is the entire fit curve. Although broad and shifted some wavenumbers, the peak positioned at  $1420\text{ cm}^{-1}$  will be disorder induced peaks which have been previously obtained in nanocrystalline diamond materials,<sup>7,8)</sup> and the broad weak peak at about  $1216\text{ cm}^{-1}$  seems to be related to  $\text{sp}^3$ -bonded amorphous carbon according to Beeman's calculations.<sup>9)</sup> The weak peak around  $1370\text{ cm}^{-1}$ , although shifted from graphite D band (at about  $1350\text{ cm}^{-1}$ ) which was often observed in CVD diamond with some variation in peak position, indicated the presence of a small quantity of  $\text{sp}^2$ -bonded amorphous carbon.

The Raman shift has been known always relate strongly to stress, with positive shift as compressive stress and negative shift as tensile stress. Figure 3 shows the correlation between distance from Silicon/Diamond interface and Raman shift. The data near Silicon/Diamond interface ranged from  $1331.5\text{ cm}^{-1}$  to  $1333.8\text{ cm}^{-1}$ , more than  $2\text{ cm}^{-1}$ . Along the distance, the data distribution range narrowed, near the Diamond/Air interface, the range was about  $1\text{ cm}^{-1}$ . From the average curve, we can see that from spot A to spot C the peak position is about

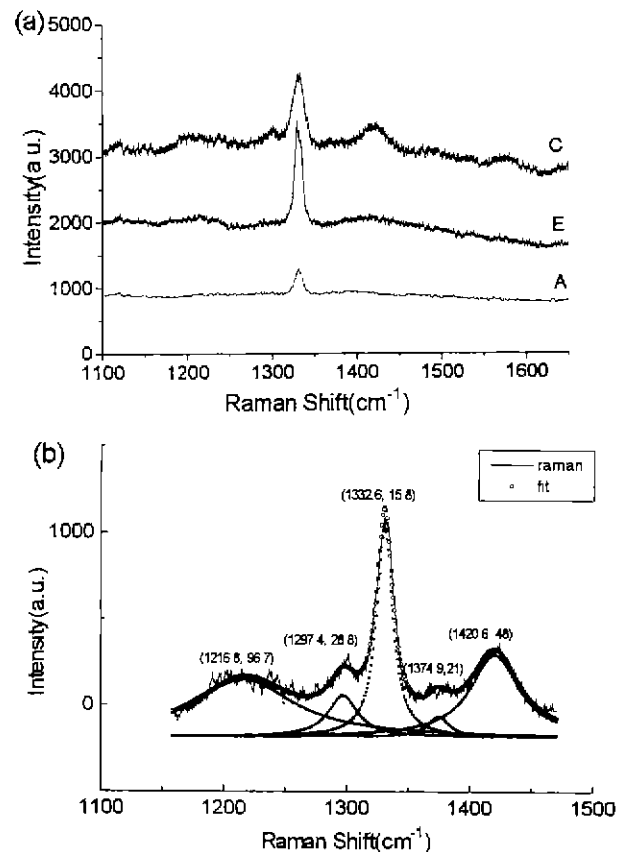
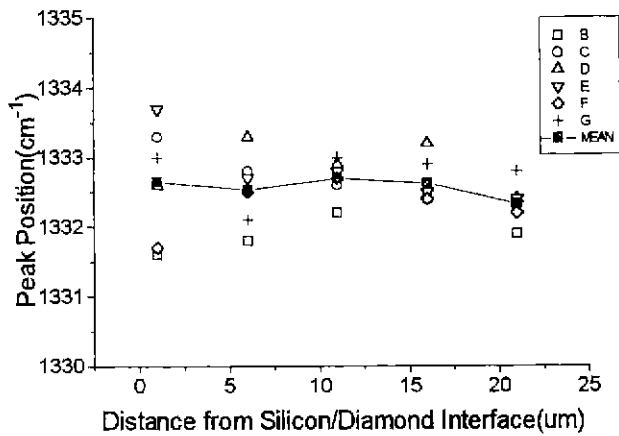


Fig. 2.(a) Typical Raman spectra at different position along cross-section of diamond film. A: close to the Silicon/Diamond interface; C: center in the film; E: close to the Diamond/Air interface. (b) Decomposition of the Raman spectrum C in Fig. 2(a), fitting data was expressed in (peak position, FWHM).



**Fig. 3.** Correlation between peak position of first order diamond Raman line and distance from Silicon/Diamond interface.

1332.5, from spot C to spot E the peak shifted to lower wave number side gradually. Even though the minimum peak shift is larger than the one of natural diamond which was used as calibration in this study. It indicates that the net stress in this sample is compressive stress, and along the distance the compressive stress reduced. According to ref. 11, we can estimate the average stress is from 0.7 to 0.4 GPa along the cross-section. Because the sample is free standing, the interfacial stress was relaxed, and thermal stress along the film was about 0.22 GPa (at ~900°C deposition temperature) according to the calculation by H. Windischmann *et al.*<sup>10</sup> The total internal stress may be due to various sources such as impurities, defects and interactions across grain boundaries.

Figure 4 is the relationship between distance from Silicon/Diamond interface and FWHM. Unlike the distribution of peak position, the FWHM distribution range changed a little along the distance from silicon to growth surface. From the average curve, we can see that at both interface the FWHM is smaller than inside. The maximum average date reached to 15 cm<sup>-1</sup> at 16 μm from Si/Diamond interface. As we know, the broadening of the Raman peak width is always relate to stress; size effect of the crystal; impurities; grain boundaries and defect sites. In another study, we have checked the depth resolution of micro-Raman spectroscopy we used, and found that the effective depth is 3-4 μm when we focus the laser spot at sample surface. Here we should point out that although we focused laser spot at the same crystal as possible as we can, we can not ignore the effect of grain boundaries and defect sites below the crystal we focused. By observing the correlation between the FWHM and Raman shift, we found it shows random distribution, no linear relationship which has been observed by L. Berman *et al.*<sup>11</sup> It indicates that the defects and impurities which caused Raman line broadening and caused Raman shift are not the same origin or only a part of them act on the Raman shift. Furthermore, the frequencies and

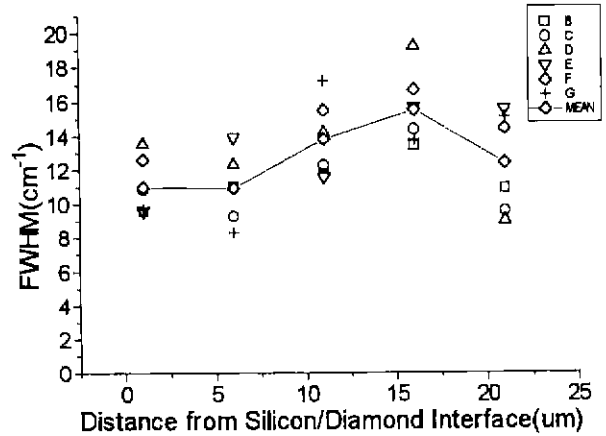


**Fig. 4.** Correlation between FWHM of first order diamond Raman line and distance from Silicon/Diamond interface.

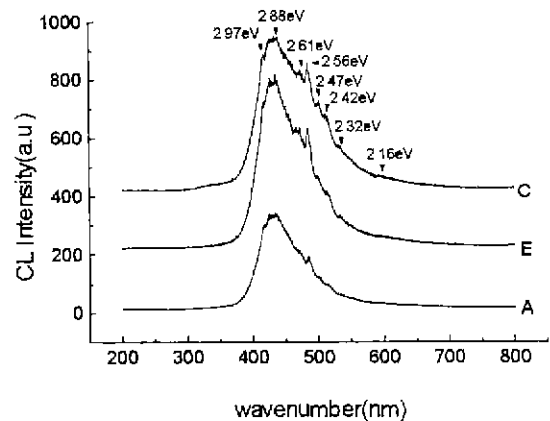


**Fig. 5.** Typical cathodoluminescence spectrum of cross-section of CVD diamond film.

asymmetric line shapes predicated by the phonon confinement model<sup>12</sup> do not agree well with our experimental data. Therefore, we suggest that phonon momentum uncertainty is of minor importance for Raman peak broadening of our sample. From Fig. 2(b) we know in the center of cross-section, there exist disorder nanocrystalline, amorphous carbon and small quantity of sp<sup>3</sup>-carbon. The possible mechanism of Raman peak's broadening of our sample is dominated by reduction of phonon lifetime due to phonon decay at grain boundaries and defect sites.

Figure 5 shows the three typical CL spectrum along the cross-section of diamond film. These spectrum are dominated by the broad band A, which is considered to be due to dislocations existing in the crystal. On the tail of band A, several weak peaks were also observed. Including 575 nm (2.16 eV) center, which involves a vacancy (or vacancies) together with a single nitrogen atom.<sup>12</sup> 2.32 eV center which is a nitrogen-vacancy complex.<sup>13</sup> 484 nm (2.56 eV) center has been found related to radiation damage.<sup>14</sup> At position A near Silicon/Diamond interface, the intensity of these small peaks is lower than that of inside. Com-

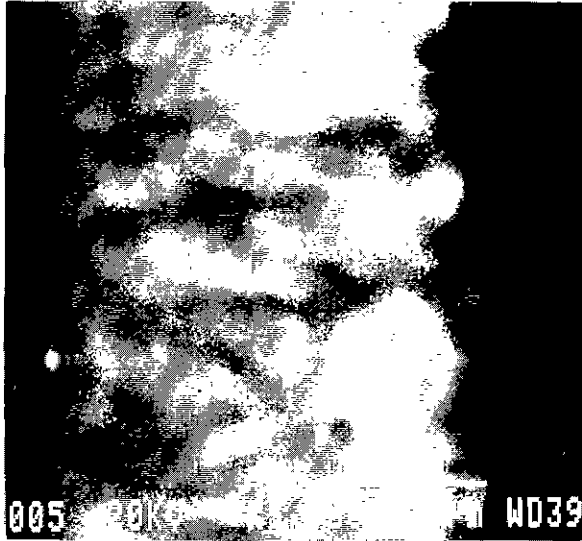


**Fig. 6.** CL image taken from cross-section of CVD diamond film.

pared with its low background Raman spectra, we suggest that defects and impurities were mainly present inside the film.

Figure 6 is the CL image of cross section sample taken with 425 nm. The difference of the luminescent region has been observed. Compared with SEM photo, the bright region is also the bright one in the second electron (SE) image. We can identify the dark region is located at grain boundaries and the location of second nucleation, but can't identify the variation of luminescent region within one particle because of the resolution of CL image.

#### IV. Conclusions

In summary, Micro-Raman spectroscopy and cathodoluminescence was employed to investigate the cross-section of diamond film. The analysis indicated that the cross-section of 24  $\mu\text{m}$  thick diamond film exhibited a type of compressive stress. Near the growth surface the compressive stress reduced to the minimum. FWHM of the first order diamond line at both Si/Diamond in-

terface and Diamond/Air interface are narrower than inside film due to high defect density, impurities and grain boundaries. In our sample, the main impurities and defects are nanocrystalline diamond, amorphous carbon, nitrogen and dislocation.

#### Acknowledgment

The authors would like to thank H. Yagi, S. Sonoda, K. Ogawa for their assistance and fruitful discussion.

#### References

1. E. Gheeraert, A. Deneuville and A. M. Bonnot, L. Abello, *Diamond and Related Materials*, 1525 (1992).
2. Nobuko S. Van Damme, Dennis C. Nagle and Stephen R. Winzer, *Appl. Phys. Lett.*, **58**[25], 2919 (1991).
3. L. J. Bernardez and K. F. McCarty, *Diamond and Related Materials*, **3**, 22 (1993).
4. Stephanie R. Sails, Derek J. Gardiner and Michael Bowden James Savage, Sajad Haq, *Appl. Phys. Lett.*, **65**[1], 43 (1994).
5. N. Yamamoto, J. C. H. Spence and D. Fathy, *Phil. Mag. B.*, **49**, 609 (1984).
6. H. Kawarada, Y. Yokota, Y. Mori, K. Nishimur and A. Hiraki, *J. Appl. Phys.*, **67**[2], 983 (1990).
7. R. J. Nemanich, J. T. Glass, G. Lucovsky and R. E. Shroder, *J. Vac. Sci. Technol.*, **A6**, 1783 (1988).
8. P. G. Buckley, T. D. Moustakas, Ling Ye and J. Varon, *J. Appl. Phys.*, **66**[8], 3595 (1989).
9. D. Beeman, J. Silverman, R. Lynds and M. R. Anderson, *Phys. Rev.*, **B30**, 870 (1984).
10. H. Windischmann and Glenn F. Epps, *J. Appl. Phys.*, **64**[4], 2231 (1991).
11. L. Bergman and R. J. Nemanich, *J. Appl. Phys.*, **78**[11], 6709 (1995).
12. J. A. Ager III, D. K. Veirs and G. M. Rosenblatt, *Phys. Rev. B*, **43**[8], 6491 (1991).
13. A. T. Collins and S. C. Lawson, *J. Phys.: Condens. Mater.*, **1**, 6927 (1989).
14. L. H. Robins, L. P. Cook, E. N. Farabaugh and A. Feldman, *Physical Rev. B*, **39**[18], 38 (1989).
15. Chemistry and Physics of Carbon, ed by Philip L. Walker, Jr and Peter A. Thrower, p. 119 (Marcel Dekker, Inc., New York and Basel).